Virology **285,** 138–152 (2001)
doi:10.1006/viro.2001.0845, available online at http://www.idealibrary.com on IDEAL®



# The HDV Large-Delta Antigen Fused with GFP Remains Functional and Provides for Studying Its Dynamic Distribution

Ko-Nien Shih and Szecheng J. Lo[1]

*Institute of Microbiology and Immunology, National Yang-Ming University, Taipei, Taiwan 11221, R.O.C.*

*Received October 19, 2000; returned to author for revision January 2, 2001; accepted January 25, 2001*

Hepatitis D virus (HDV) requires the isoprenylated large delta antigen (LDAg) for interaction with hepatitis B surface antigen (HBsAg) to allow packaging and secretion out of the host cell. Phosphorylated LDAg has been found but, as yet, neither localization of LDAg within the nucleus nor any other function has been correlated with modification. In this study, we transfected HuH-7 or HeLa cells with plasmids encoding various lengths of LDAg [designated GFP–LD and GFP–LD(31-214) for full length and a deletion, respectively] or non-isoprenylated mutants of these [designated GFP–LDM and GFP–LD(31-214)M] fused to the green fluorescent protein (GFP). These fusion proteins were then characterized and it was found that: (i) the addition of the GFP did not interfere with the functioning of the full-length or N-terminally deleted LDAgs when interacting with HBsAg for secretion; (ii) the HDV small antigen (SDAg) together with the GFP–LD, but not the GFP–LD(31-214), could be cosecreted by HBsAg; and (iii) the GFP–LD, but not the GFP–LD(31-214), exerted a dominant-negative role on HDV genome replication. Analyses of transiently transfected cells and postmitotic permanent cells revealed the sequential appearance of GFP–LD in the nucleoplasm, then in the nucleolus, and finally in nuclear speckles (NS). Isoprenylation of LDAg seems to be important for targeting to and accumulating in the NS, which was evident from the dynamic and static localization of the non-isoprenylation mutant (GFP–LDM) and the distribution of wild-type (GFP–LD) when treated with an isoprenylation inhibitor, lovastatin, for more than 48 h. Permanently expressing GFP–LD cells allowed us to show the dynamic redistribution of dephosphorylated GFP–LD from the nucleolus to the SC-35 containing NS in the presence of dichlororibofuranosyl benzimidazole (DRB) and then the translocation back of the GFP–LD to the nucleolus within 2 h after removal of DRB. Our studies thus suggest that the various versions of the GFP–LD fusion protein, having the same function as their nonfusion counterparts, can be a powerful tool for the study of the dynamic localization of LDAg when correlated with the functional modification of this protein. 

## INTRODUCTION

Hepatitis D virus (HDV) was discovered as an agent associated with severe liver injury in individuals already infected with hepatitis B virus (HBV) (Rizzeto, 1983). In fact, HDV is a subviral satellite and requires HBV to supply envelope proteins (HBsAg) for its packaging, secretion, and infection (Ponzetto *et al.,* 1984; Bonino *et al.,* 1986). In addition to the HBsAgs, the virion particle of HDV contains its own genome and two isoforms of the HDV encoded antigens (HDAg), the small delta antigen (SDAg) and the large delta antigen (LDAg) (for a review see Lai, 1995, and references therein). The HDV genome comprises a 1.7-kb single-stranded circular RNA molecule that is approximately 70% self-complementary and forms a highly base-paired rod-like structure (Chen *et al.,* 1986; Wang *et al.,* 1986; Kos *et al.,* 1986; Makino *et al.,* 1987). The SDAg is encoded by an open reading frame (ORF) of HDV anti-genome, contains 195 amino acids, and produces a protein of 24 kDa (Wang *et al.,* 1986; Weiner *et al.,* 1988). LDAg, which has a molecular weight of 27,000, consists of the same 195 amino acids as the SDAg with an additional 19 amino acids at the C-terminus, which results from RNA editing and converts an amber stop codon (UAG) to a tryptophan codon (UGG) during the HDV genome replication cycle (Luo *et al.,* 1990; Casey *et al.,* 1992; Zheng *et al.,* 1992).

Although the two HDAgs share a common 195-amino-acid sequence, they have opposing biological functions in the HDV life cycle. The SDAg is an essential factor for HDV RNA replication (Kuo *et al.,* 1989), while the LDAg is a dominant repressor for replication (Kuo *et al.,* 1989; Chao *et al.,* 1990) and, crucially, is required for interaction with HBsAg for packaging and secretion (Chang *et al.,* 1991; Ryu *et al.,* 1992). Both HDAgs have been demonstrated to be phosphoproteins (Chang *et al.,* 1988; Hwang *et al.,* 1992; Yeh *et al.,* 1996; Bichko *et al.,* 1997; Mu *et al.,* 1999), with phosphorylation of SDAg at serine-2, but not of LDAg, being important for HDV RNA replication (Yeh *et al.,* 1996). Since the SDAgs can be phosphorylated at both serine and threonine while the LDAg can be phosphorylated only at serine, this may account for their distinct biological functions (Mu *et al.,* 1999). Only the LDAg contains an

[1] To whom correspondence and reprint requests should be addressed. Fax: 886-2-28212880. E-mail: losj@ym.edu.tw.

0042-6822/01 $35.00

isoprenylation signal at the C-terminus and mutation of an isoprenylation site or deletion of 15 amino acids upstream of the isoprenylation site abolishes the assembly and secretion function of LDAg (Glenn *et al.,* 1992; Lee *et al.,* 1994, 1995). The SDAg alone cannot be secreted with HBsAg (Chang *et al.,* 1991; Wang *et al.,* 1991; Lazinski and Taylor, 1993), but is secreted in the presence of LDAg, indicating a direct interaction between SDAg and LDAg (Chang *et al.,* 1992; Lazinski and Taylor, 1993; Sheu *et al.,* 1996).

Several lines of evidence indicated that the interaction between SDAg and LDAg is important for HDV replication, assembly, and secretion (Ryu *et al.,* 1992; Xia and Lai, 1992; Chang *et al.,* 1993; Wang *et al.,* 1994). The coiled-coil domain at the N-terminus of HDAgs is required for the interactions that exert activation or inhibition functions (Lazinski and Taylor, 1993). Other functional domains of HDAgs, such as RNA-binding, nuclear targeting, and nucleolin-binding sites, are well mapped and characterized (for a review see Lai, 1995; Chang *et al.,* 1995; Lee *et al.,* 1998). The distribution of SDAg and LDAg inside of transfected cells, with or without the presence of the whole HDV genome, has been studied by immunofluorescence to reveal the pattern in the nucleoplasm, the nucleolus, the SC35-containing speckles, and the Golgi complex (Xia *et al.,* 1992; Wu *et al.,* 1992; Chang *et al.,* 1992; Bichko and Taylor, 1996). By using anti-farnesyl antibody, the isoprenylated LDAg can be localized in the nucleolus (Lin *et al.,* 1999). However, correlation of the distribution of HDAgs with their modification and function remains largely unknown.

In the past few years, many studies have shown that the green fluorescent protein (GFP) from jellyfish is a popular tool for localization of a specific protein distribution inside cells when the GFP is fused with that particular protein (Misteli and Spector, 1997; White and Stelzer, 1999). Many GFP–fusion proteins are found to retain all the functions of their authentic proteins and are nontoxic to cells. Thus GFP fusion can be used for the study of dynamic change inside cells as was done with protein kinase C and coilin (Sakai *et al.,* 1997; Boudonck *et al.,* 1999). In this study, we fused a full-length LDAg with GFP (GFP–LD) and created three mutants, including the non-isoprenylation mutant (GFP–LDM), deletion mutant [GFP–LD(31-214)], and double mutant of the deletion and non-isoprenylation form [GFP–LD(31-214)M]. This system allowed us to detect the dynamic distribution of LDAgs inside the nucleus when LDAgs are isoprenylated/non-isoprenylated or phosphorylated/dephosphorylated, and to our knowledge, this is the first report showing how the distribution of LDAg in various locations correlates with its modification.

## RESULTS

### Various forms of LDAg fused with GFP produce different nuclear distribution patterns

To visualize a dynamic distribution of LDAg in living cells, we constructed plasmids of the wild-type and an N-terminally truncated mutant (deleted for amino acids 1 to 30) of LDAg fusing to the C-terminus of GFP and designated pGFP–LD and pGFP–LD(31-214), respectively. Two other closely related plasmids, pGFP–LDM and pGFP–LD(31-214)M, were also created by mutation of the isoprenylation site of pGFP–LD and pGFP–LD(31-214). The distribution of these GFP–fusion proteins was examined during transient transfection of these plasmids into HuH-7 or HeLa cells for 3 days posttransfection and on permanent expression in HeLa cells. A unique distribution pattern was observed for each fusion protein, either during transient transfection or on permanent expression. The unique distribution pattern for each fusion protein was similar in cells of both hepatic (HuH-7) and nonhepatic (HeLa) origin.

Four different permanently transfected HeLa cells were obtained by transfection of pGFP–LD, pGFP–LDM, pGFP–LD(31-214), and pGFP–LD(31-214)M. We correlated the distribution pattern of the GFP–fusion proteins with their location in the cells by staining with anti-nucleolin, a prominent marker for the nucleolus, and the DNA dye Hoechst 33258. The GFP–LD in HeLa cells appeared in both the nucleolus and the nuclear speckles (NS) (Figs. 1A, 1B, and 1C). The latter varied in size (0.1–3 $\mu$m) and number (3–30) (Fig. 1A). The colocalization of GFP–LD and nucleolin (Fig. 1C) was similar to that of authentic LDAg and nucleolin (data not shown, Lee *et al.,* 1998). An even distribution pattern of GFP–LD, instead of a prominent nucleolus and NS pattern, was observed in a dividing cell (the left center cell shown in Fig. 1A). In cells expressing the non-isoprenylation fusion protein GFP–LDM, the green fluorescent signals (Fig. 1E) were present mostly in the nucleolus (Figs. 1F and 1G). Occasionally, the GFP–LDM protein was also observed in the nuclear speckles, which were larger and fewer than 5 in number (Fig. 1E) compared to the wild-type GFP–LD (Fig. 1A). Unlike the full-length GFP–LD/GFP–LDM expression patterns, the patterns of distribution of GFP–LD(31-214) and GFP–LD(31-214)M were very similar, with an even distribution in the nucleoplasm including the nucleolus (Figs. 1I and 1M). Interestingly, the distribution of nucleolin in some stably expressing cells was changed from an oval-rounded form into an irregular form (Figs. 1J and 1N).

### N-terminal deletion mutants of LDAg have a lower density than full-length versions in the sucrose gradient

To know whether the different distribution pattern of LDAg fusion proteins was due to an inability to form

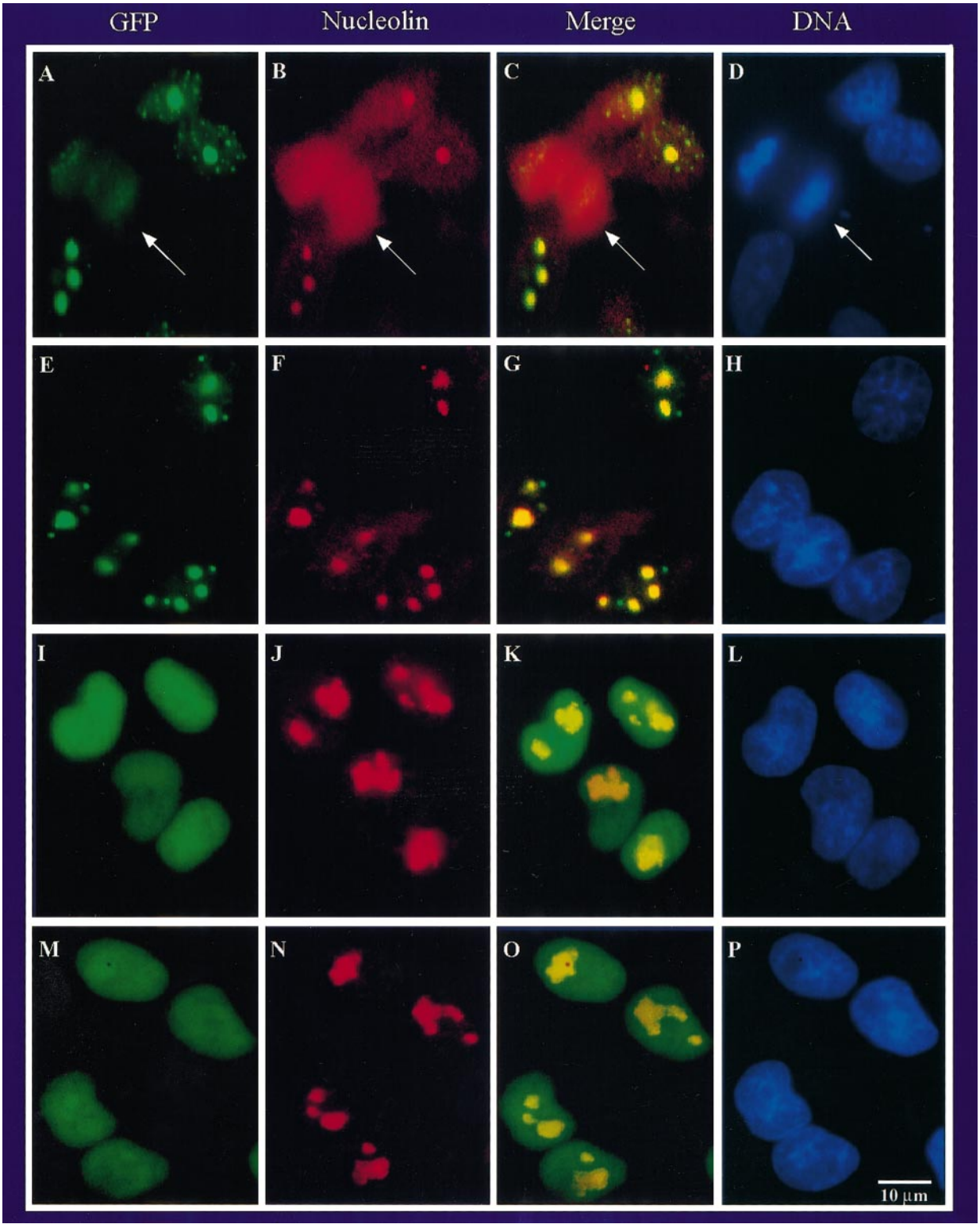


FIG. 1. Fluorescence pattern of various forms of LDAg fused with the green fluorescent protein (GFP) in permanently transfected HeLa cells. (A–D) GFP–LD; (E–H) GFP–LDM; (I–L) GFP–LD(31-214); (M–P) GFP–LD(31-214)M. Pictures in the first (leftmost) column were obtained using a fluorescence microscope with a FITC filter and show the GFP pattern (A, E, I, and M). The pictures in the second column show cells stained with anti-nucleolin antibody and a secondary antibody conjugated with rhodamine (B, F, J, and N). The third column shows the merged pictures from the first and second columns (C, G, K, and O). The yellow color indicates the colocalization of GFP–fusion protein with nucleolin. The fourth column shows cells stained with DNA dye to outline the morphology of the nucleus (D, H, L, and P). A dividing cell is indicated by an arrow. All pictures were taken at the same magnification as indicated by the 10-$\mu$m bar in P.

multimers or an inability to interact with different cellular factors that resulted in forming complexes of various densities, we performed sucrose density analysis. The nuclear extracts from permanently expressing HeLa cells were subjected to centrifugation on a 10–50% sucrose gradient. The presence of GFP–fusion protein in each density fraction was analyzed by SDS–PAGE followed by Western blot detection using anti-HDAg antibody. For a comparison, some blots were also probed with anti-nucleolin. As is characteristic of nucleolin, it was widely distributed in various density fractions (fractions 3 to 18), although there were two peaks, one at lower density (fractions 3–8) and other at a higher density (fractions 14–18) (Fig. 2A). The broad distribution of nucleolin was similar in the coexpression with GFP–LD or with authentic LDAg (Huang *et al.,* 2001). In contrast, the GFP–LD with an expected molecular mass of 57 kDa had a less broad distribution, from fractions 7 to 18 (1.35 to 1.80 g/ml), and was concentrated mostly in fractions 8 and 9 (1.40 to 1.44 g/ml) (Fig. 2B). Nevertheless, the coexistence of nucleolin and GFP–LD in the lower part of the gradient (fractions 14–18) suggested that GFP–LD and nucleolin might form a complex or be associated (Lee *et al.,* 1998) and present in the nucleolus as shown in Fig. 1C. The GFP–LDM with a molecular weight similar to that of GFP–LD showed a slightly different distribution pattern, being distributed from fractions 9 to 18 (1.44 to 1.80 g/ml) with the highest concentration in fraction 9 (Fig. 2C). Whether these minor differences between GFP–LD and GFP–LDM were due to their prenylation state or due to an association with some cellular factors is unclear. GFP–LD(31-214) and GFP–LD(31-214)M, which has a molecular mass of around 54 kDa, showed similar distributions between fractions 3 and 8 (1.20 to 1.30 g/ml) (Figs. 2D and 2E). The reason that both deletion proteins were not present in the heavier fractions, as were their full-length counterparts, may be truncation of these proteins' coiled-coil domain. Although the density of the two deletion mutants was lower than that of the full-length versions, the deletion mutants could also self-associate or bind different cellular factors, since their density was equivalent to a molecular mass of around 150 kDa, significantly heavier than their expected molecular mass of 54 kDa.

### GFP fusion of the full-length or N-terminal deletion of LDAg in an isoprenylated form is able to be cosecreted with HBsAg

Previously, the LDAg has been demonstrated to be packed and secreted by HBsAg (Wang *et al.,* 1991; Chen *et al.,* 1992). To test whether the GFP–fusion proteins still retain such biological activity, we cotransfected plasmids expressing the various fusion proteins with an HBsAg expression plasmid. Medium from 3 and 6 days posttransfection was collected and analyzed for the presence of GFP–fusion protein. Western blot analysis showed that both GFP–LD and GFP–LD(31-214) were secreted by the HBsAg as authentic LDAgs (Fig. 3B, lanes 2, 4, and 6), but neither of the nonprenylation mutants, GFP–LDM and GFP–LD(31-214)M, were secreted (Fig. 3B, lanes 5 and 7). Intracellular analyses showed that GFP–LDM and GFP–LD(31-214)M were indeed expressed inside the transfected cells (Fig. 3A, lanes 5 and 7). Taking these results together, we concluded that the addition of GFP prior to that of the LDAg did not interfere with its biological function of secretion by HBsAg. This is consistent with previous reports that the coiled-coil domain is not required for LDAg secretion while isoprenylation is so required (Chen *et al.,* 1992; Sheu *et al.,* 1996).

### GFP–LD(31-214) loses the capability to interact with SDAg for secretion with HBsAg

It has been shown that the SDAg alone cannot be packed into HBsAg particles except in the presence of LDAg (Wang *et al.,* 1991; Sheu *et al.,* 1996). To examine whether the secretable GFP–LD and GFP–LD(31-214) still have the ability to cosecrete SDAg, we cotransfected plasmids expressing the SDAg (pMTSD) and the GFP–LD or GFP–LD(31-214) [pGFP–LD or pGFP–LD(31-214)] with the plasmid expressing the HBsAg (pMTS). Western analyses showed that the SDAg coexisted with various forms of LDAgs inside the transfected cells (Fig. 4A, lanes 3 to 5). However, the collected media showed that wild-type GFP–LD but not the N-terminally truncated mutant GFP–LD(31-214) can cosecrete SDAg (Fig. 4B, lane 5 vs lane 4). It has been demonstrated that the N-terminal leucine zipper motif (amino acids 29–56) of HDAg participates in the interaction of LDAg and SDAg during virion assembly (Lai, 1995). The current data suggest that the N-terminal 30-amino-acid deletion may disrupt the structure of the leucine zipper motif and the result is the loss of interaction between GFP–LD(31-214) and SDAg during HBsAg particle assembly (Moraleda *et al.,* 1999).

### HDV RNA replication is inhibited by the full-length GFP–fusion proteins but not the N-terminal deletion mutants

To determine whether the GFP–LDAg fusion proteins exhibit the *trans*-dominant inhibition of authentic LDAg on HDV RNA replication, we transfected pCMVDag2, a CMV promoter driving replication-competent dimer of 1.7-kb HDV cDNA, into the stable cells that constantly express GFP–LD, GFP–LDM, GFP–LD(31-214), or GFP–LD(31-214)M. After 6 days posttransfection, cells were lysed and HDV RNA was analyzed by Northern blot. As shown in Fig. 5A, HDV RNA replication was almost completely inhibited in the GFP–LD and GFP–LDM expres-

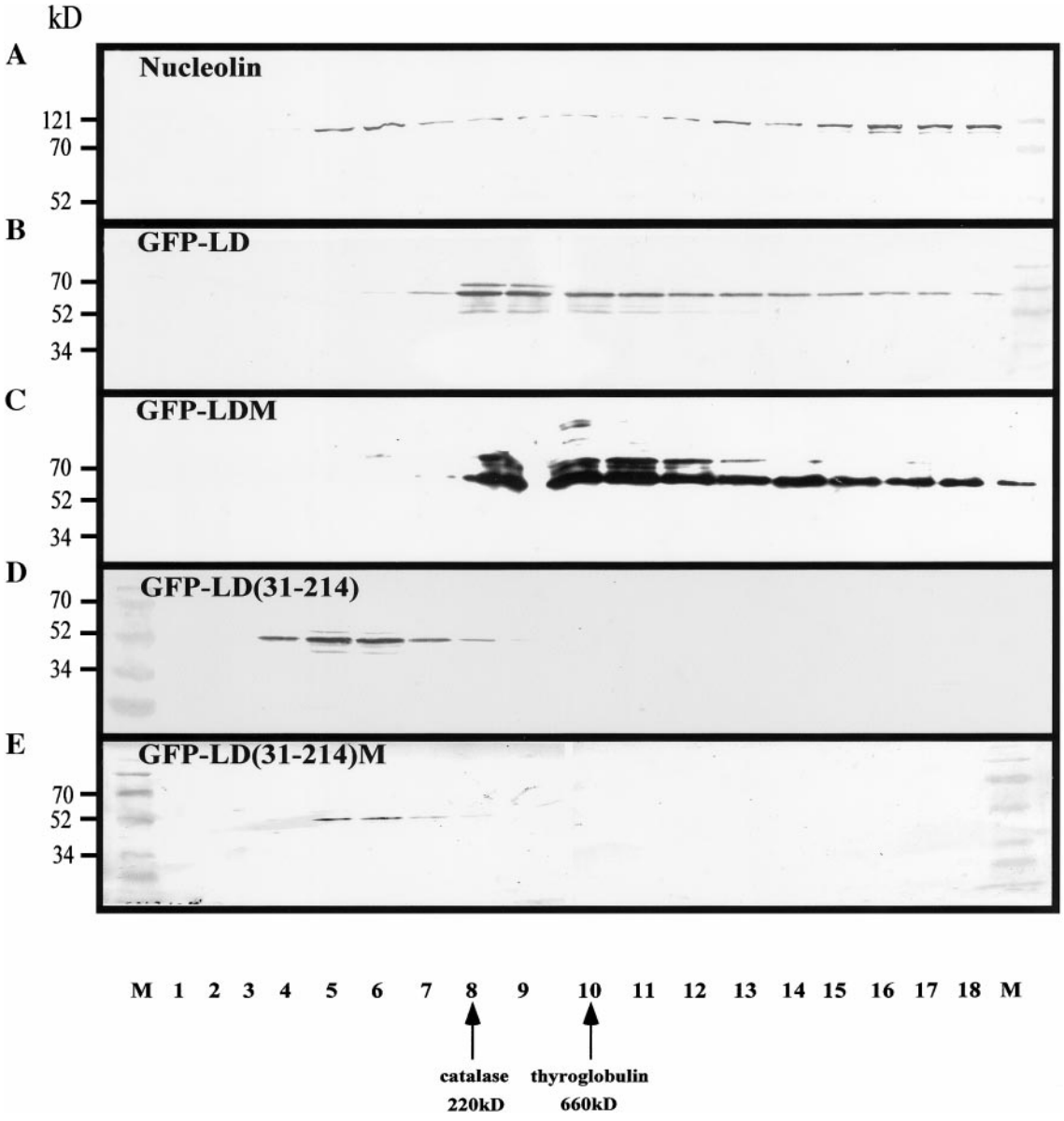


FIG. 2. Sucrose density gradient analysis of various GFP–LDAg fusion proteins. The nuclear extracts of permanent transfection HeLa cells were subjected to a 10 to 50% discontinuous sucrose gradient. The gradients were fractionated into 18 tubes from the top to bottom. The distribution of nucleolin from the GFP–LD cells was analyzed by anti-nucleolin antibody (A). The GFP–LDAgs from four different stable cell lines were detected using anti-HDAg antibody and are shown in (B) GFP–LD, (C) GFP–LDM, (D) GFP–LD(31-214), and (E) GFP–LD(31-214)M. The number (1–18) indicates the fractions from the top to the bottom of the gradient. The catalase is 220 kDa and thyroglobulin is 660 kDa; these were used as fractionation markers and are located in fractions 7 and 10, respectively. The protein standard markers for SDS–PAGE are indicated to the left of each panel.

sion cells (lanes 6 and 7), but not in the GFP–LD(31-214) and GFP–LD(31-214)M cells (lanes 4 and 5). The inhibition results obtained for full-length LDAgs were supported by the evidence from loading an internal control with an equal amount of RNA at a similar transfection efficiency and the resultant production of HDAg (Figs. 5B, 5C, and 5D). These data suggest that the deletion of N-terminal LDAg has resulted in loss of an essential domain for the inhibition of HDV RNA replication and the LDAg fusion with GFP does not mask the conformation that causes *trans*-inhibition.

### An inhibitor of isoprenylation decreases the nuclear speckle distribution of GFP–LDAg

Since the nuclear distribution between GFP–LD and GFP–LDM differed in the number of NS (Fig. 1A vs 1E), we attempted to verify whether isoprenylation was a factor in LDAg targeting to and accumulating in NS. We treated both the GFP–LD and the GFP–LDM permanently expressing cells with a mevalonate synthesis inhibitor, lovastatin (Sinensky *et al.,* 1990; Ivessa *et al.,* 1997), which results in the inhibition of isoprenylation. After 48 h

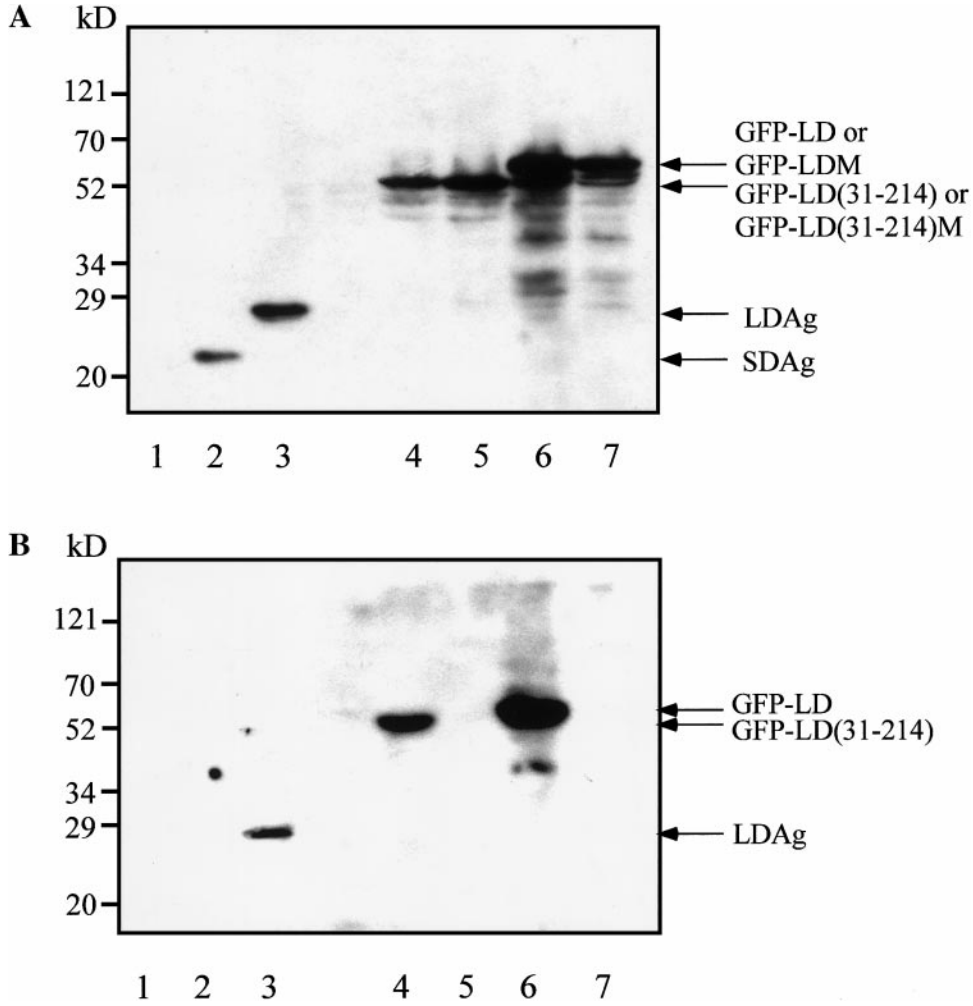


FIG. 3. Western blot analysis of the secretion capability of the GFP–LDAg fusion protein with HBsAg. Various plasmids encoding HDAg were cotransfected with an HBsAg expressing plasmid into human hepatoma cells, HuH-7. Six days posttransfection, the intracellular (A) and secretion (B) proteins were analyzed using anti-HDAg antibodies. The predicted size of each LDAg protein is indicated on the right and the protein standard markers are indicated on the left. Lane 1 shows a mock transfection. Other transfected plasmids, in addition to the plasmid expressing HBsAg, are as follows: pMTSD (lane 2), pMTLD (lane 3), pGFP–LD(31-214) (lane 4), pGFP–LD(31-214)M (lane 5), pGFP–LD (lane 6), and pGFP–LDM (lane 7).

of lovastatin treatment, the nucleoplasmic pattern of GFP–LD changed, with the numbers of NS being reduced compared with untreated cells or cells treated for 24 to 36 h (Fig. 6D vs Figs. 6A, 6B, and 6C). Almost no speckle pattern could be observed when the GFP–LD cells were treated with lovastatin for 60 h (Fig. 6E) compared with the GFP–LD cells incubated in the control medium for 60 h (Fig. 6F). In contrast, the distribution pattern for GFP–LDM was similar in both treated and untreated cells, where it appeared in the nucleolus with little or no speckle pattern (data not shown). These results suggest that the isoprenylation of GFP–LD is a modification that may cause the protein to localize to the NS.

### Sequential distribution and accumulation of GFP–LD observed in various sites of the nucleus

The advantage of using a GFP–fusion protein is that the dynamic location of the protein can be followed in living cells. It is possible for us to trace the sequential distribution of GFP–LD through the cell. After 8 h posttransfection, the GFP–LD was observed inside the nucleus, appearing with an even distribution pattern (Fig. 7A). Thereafter, up to 20 h posttransfection, the GFP–LD appeared in the nucleolus and remained in the nucleoplasm (Fig. 7A). After 36 h posttransfection, although the distribution of GFP–LD was not synchronized in every transfected cell, the speckle pattern of LDAg became obvious (Fig. 7A). A prominent speckle and nucleolus distribution of GFP–LD were easily observed after 48 h posttransfection (Fig. 7A) and the pattern was similar to that seen in the permanently expressing cells (Fig. 1A). The redistribution of GFP–LD was also detected in the permanently expressing cells, which were at a point in the cell cycle right after the mitosis stage. As shown in Fig. 7B, the sequential distribution of GFP–LD seemed to be nucleoplasm → nucleolus → NS. Combining the results of the transient transfection and the postmitosis

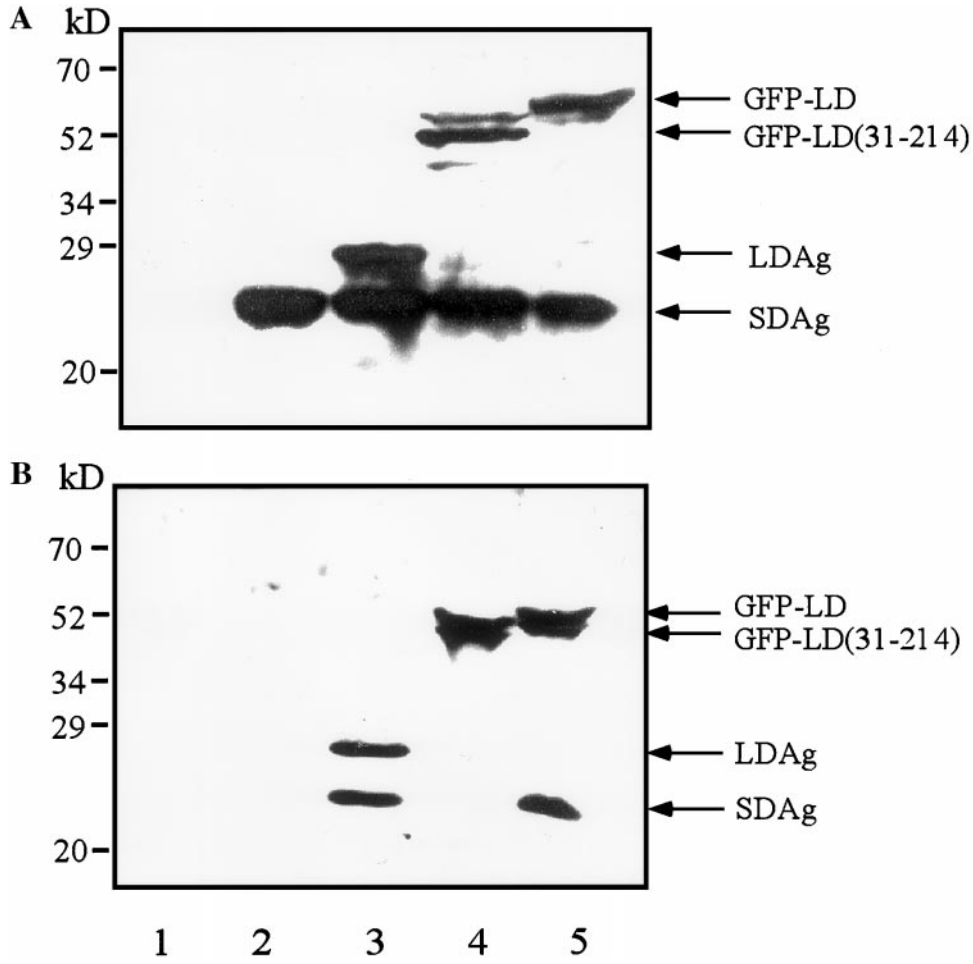


FIG. 4. Western blot analysis of the cosecretion of SDAg with various GFP–LDAg fusion proteins and HBsAg. Plasmids encoding the various forms of LDAg were cotransfected with pMTS expressing HBsAg and pMTSD expressing SDAg into human hepatoma cells, HuH-7. Six days posttransfection, the intracellular (A) and secretion (B) proteins were analyzed using anti-HDAg antibody. The predicted size of each LDAg protein is indicated on the right and the protein standard markers are indicated on the left. Lane 1 shows a mock transfection. In addition to the transfected pMTS plasmids, other plasmids used in each transfection are as follows: pMTSD (lane 2), pMTSD + pMTLD (lane 3), pMTSD + pGFP–LD(31-214) (lane 4), and pMTSD + pGFP–LD (lane 5).

of permanent cells suggested that the specific localization of GFP–LD in various structures may be dependent on its conformation when associated with a particular nuclear protein.

### Redistribution of GFP–LD between the nucleolus and SC-35 containing NS by DRB treatment

Previously, the LDAg has been demonstrated to show a 50% reduction in phosphorylation in the presence of the casein kinase II (CKII) inhibitor, dichlororibofuranosyl benzimidazole (DRB) (Yeh *et al.,* 1996). We were therefore interested to know whether the distribution of GFP–LD would be changed when cells were treated with DRB. As shown in Fig. 8, after 1 h of treatment with DRB, the GFP–LD in the nucleolus was concentrating in a few spots and the number of NS had increased. After 2 h, GFP–LD was mainly in NS and very little remained in the nucleolus (Fig. 8C). When DRB was removed for 1 h, GFP–LD remained largely in NS (Fig. 8D). However, 2 h postremoval of DRB, the GFP–LD relocated back to the nucleolus (Fig. 8E). The most interesting feature is that each cell retained the same number of nucleoli as before DRB treatment. In order to identify the nature of the NS that the GFP–LD targets to, we stained with anti-SC 35 antibody cells treated with or without DRB. As shown in Fig. 9, in untreated cells, GFP–LD was in the nucleolus and in small NS (Fig. 9A) and only a small portion of GFP–LD ($<1\%$) was colocalized with SC-35 in the NS (Fig. 9C). However, after cells were treated with DRB for 2 h, GFP–LD was present in NS only and 90% of the GFP–LD costained with SC-35 (Fig. 9G).

## DISCUSSION

The role and function of LDAg in the HDV replication cycle have been largely explored in the past decade, including its subdomain, modification, and distribution

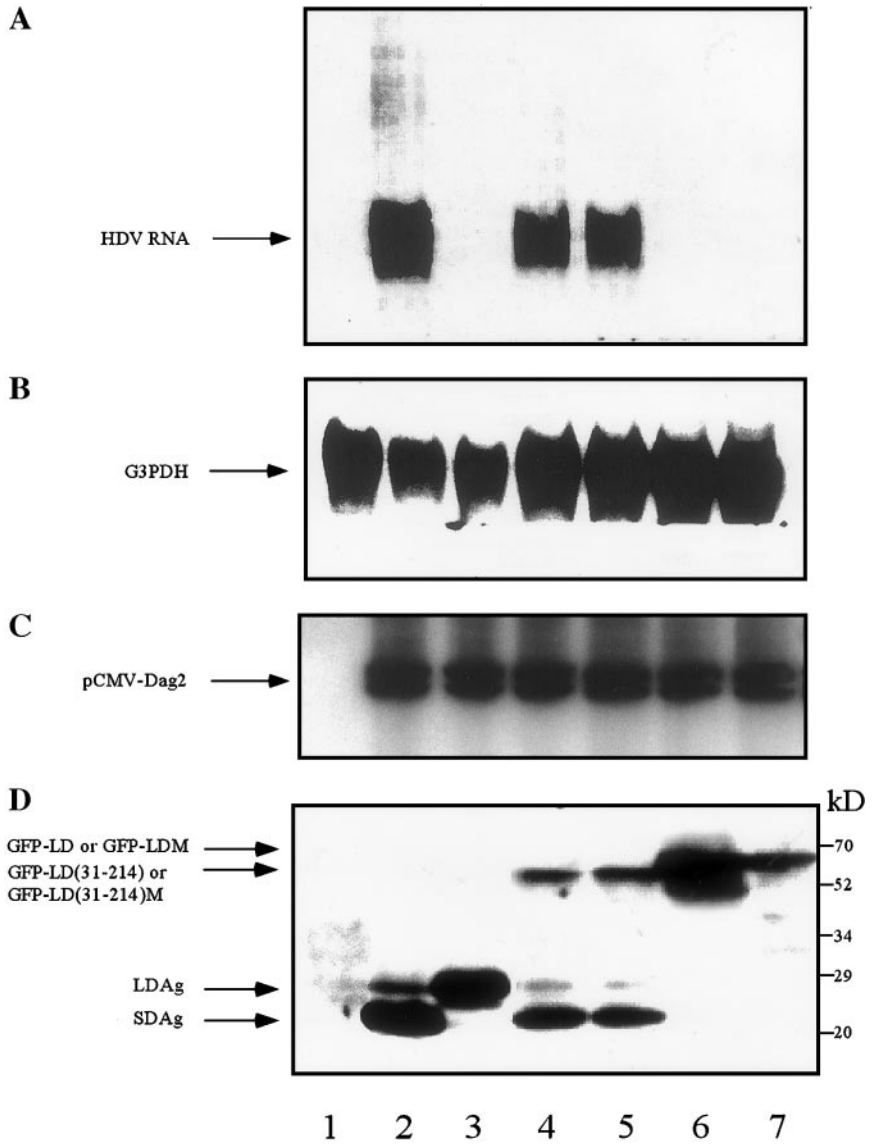


FIG. 5. Inhibition of HDV genome replication in HeLa cells expressing various GFP–fusion proteins. (A) Northern blot analysis of the intracellular HDV RNA genome. (B) Northern blot analysis of cellular G3PDH expression. (C) Southern blot analysis of transfected plasmid, pCMVDag2, which indicated transfection efficiency. (D) Western blot analysis of the intracellular HDAg. The predicted migration positions of RNA, DNA, or protein are indicated to the left of each panel. Protein standard markers are shown on the right of D. Lane 1 is a mock transfection of HeLa. Lane 2: the cotransfection of pCMVDag2 and pMTSD into HeLa cells. Lane 3: cotransfection of pCMVDag2 and pMTLD into HeLa cells. Lanes 4 to 7 show the cotransfection of pCMVDag2 and pMT into HeLa cells constantly expressing GFP–LD(31-214) (lane 4), GFP–LD(31-214)M (lane 5), GFP–LD (lane 6), and GFP–LDM (lane 7).

inside of the nucleus (Kuo *et al.,* 1989; Chao *et al.,* 1990; Chang *et al.,* 1991, 1995; Ryu *et al.,* 1992; Glenn *et al.,* 1992; Lee *et al.,* 1994; Yeh *et al.,* 1996; Wu *et al.,* 1992; Lin *et al.,* 1999). Very recently, LDAg location at the promyelocytic leukemia protein (PML)-containing speckles with the HDV anti-genome has well been studied (Bell *et al.,* 2000). However, the following events, (i) location of LDAg when inhibition of HDV RNA replication occurs, (ii) the location of assembly with SDAg and the HDV genome to form RNP, and (iii) the interaction with HBsAg to form viral particles, are less well defined. By using the powerful tool of GFP in this study, we are able to demonstrate the translocation of LDAg between the nucleolus and various nuclear speckles when it is modified in different ways, either by isoprenylation or by phosphorylation. In addition, we have demonstrated that the addition of GFP to the N-terminal of LDAg does not alter any of the known functions of LDAg. Although an ectopic addition (Ras) on LDAg has been shown not to interfere with LDAg secretion (Lee *et al.,* 1995), the GFP–LD in this study has the longest addition as yet that retains all three different functions of LDAg.

Another novel finding in this study is the linking together of the distribution, biochemistry, and function of

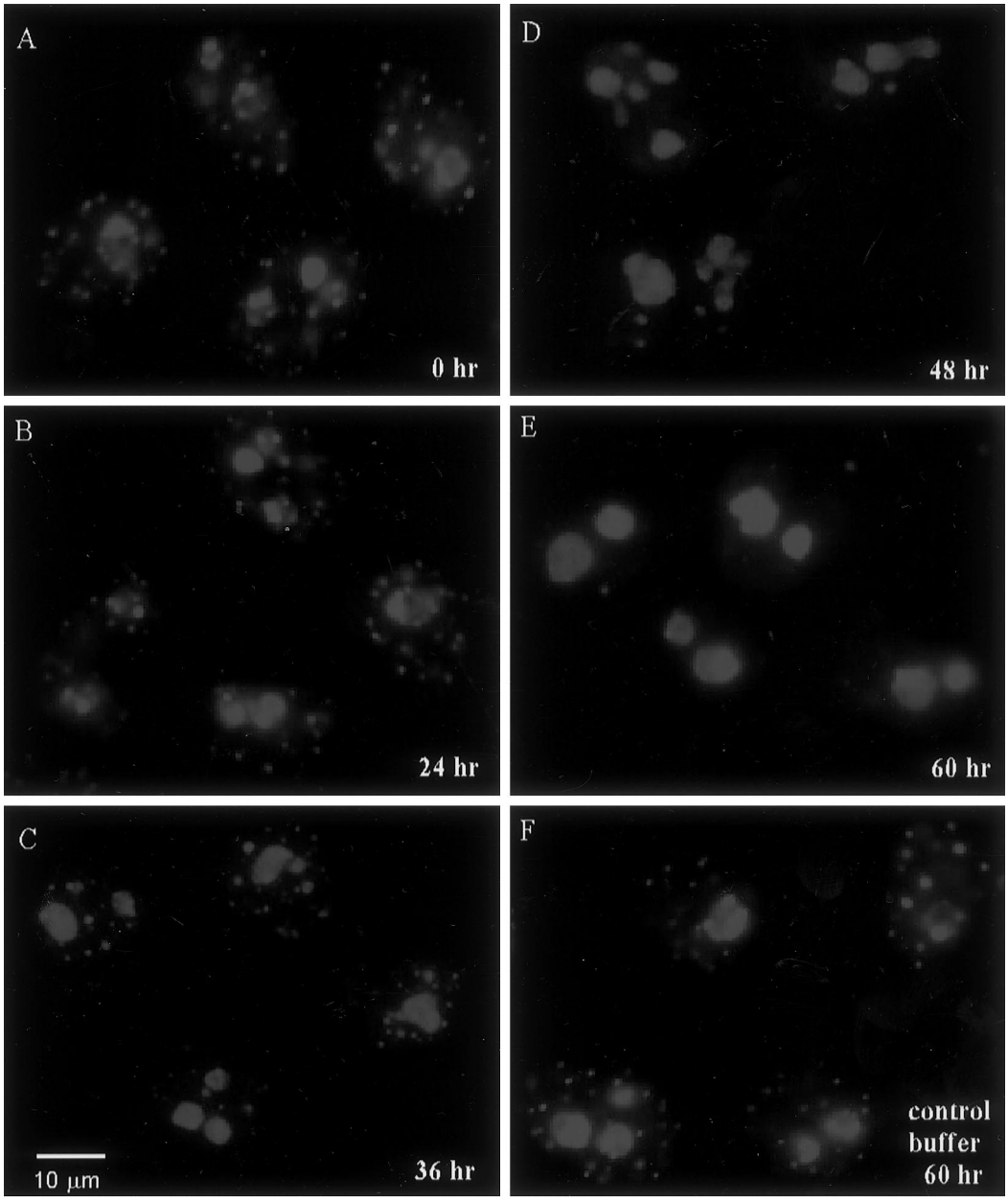


FIG. 6. Fluorescence pattern of GFP–LD distribution after lovastatin treatment. The permanently expressing GFP–LD cells were treated with 50 $\mu$M lovastatin for (A) 0, (B) 24, (C) 36, (D) 48, or (E) 60 h. Cells were incubated in a control buffer for 60 h (F). The scale bar represents 10 $\mu$m.

LDAg. Although the importance of the coiled-coil domain at the N-terminal LDAg for oligomerization has been demonstrated (Xia and Lai, 1992; Wang and Lemon, 1993; Zuccola *et al.,* 1998), we are the first to use a sucrose gradient to separate the complex containing LDAg into various densities and to show that the N-terminally truncated protein forms a lower density complex (Figs. 2C and 2D). This can be interpreted as showing that the coiled-coil domain is important not only for LDAg self-oligomerization but that it also plays a part in the interaction with factors that are present in the nucleolus, such as nucleolin (Figs. 1C and 1G vs 1K and 1O). Very recently, Grosset *et al.* (2000) used the sucrose density gradient method to demonstrate that five proteins (Unr, PABP, PAIP-1, NSAP1, and hnRNP D) exist as a complex. We thus suggest that the sucrose density separation method is an alternative choice, other than the method of yeast two-hybrid and coimmunoprecipitation, to search for HDAg-associated proteins.

In addition to the previous study showing the direct binding of HDAg and nucleolin (Lee *et al.,* 1998), the current study indicated that the GFP–LD and GFP–LDM might form various density complexes with the nucleolin and present mainly in the nucleolus (Figs. 1 and 2). Since the GFP–LD(31-214) and GFP–LD(31-214)M appear in the nucleoplasm homogeneously (Fig. 1) and they lost the

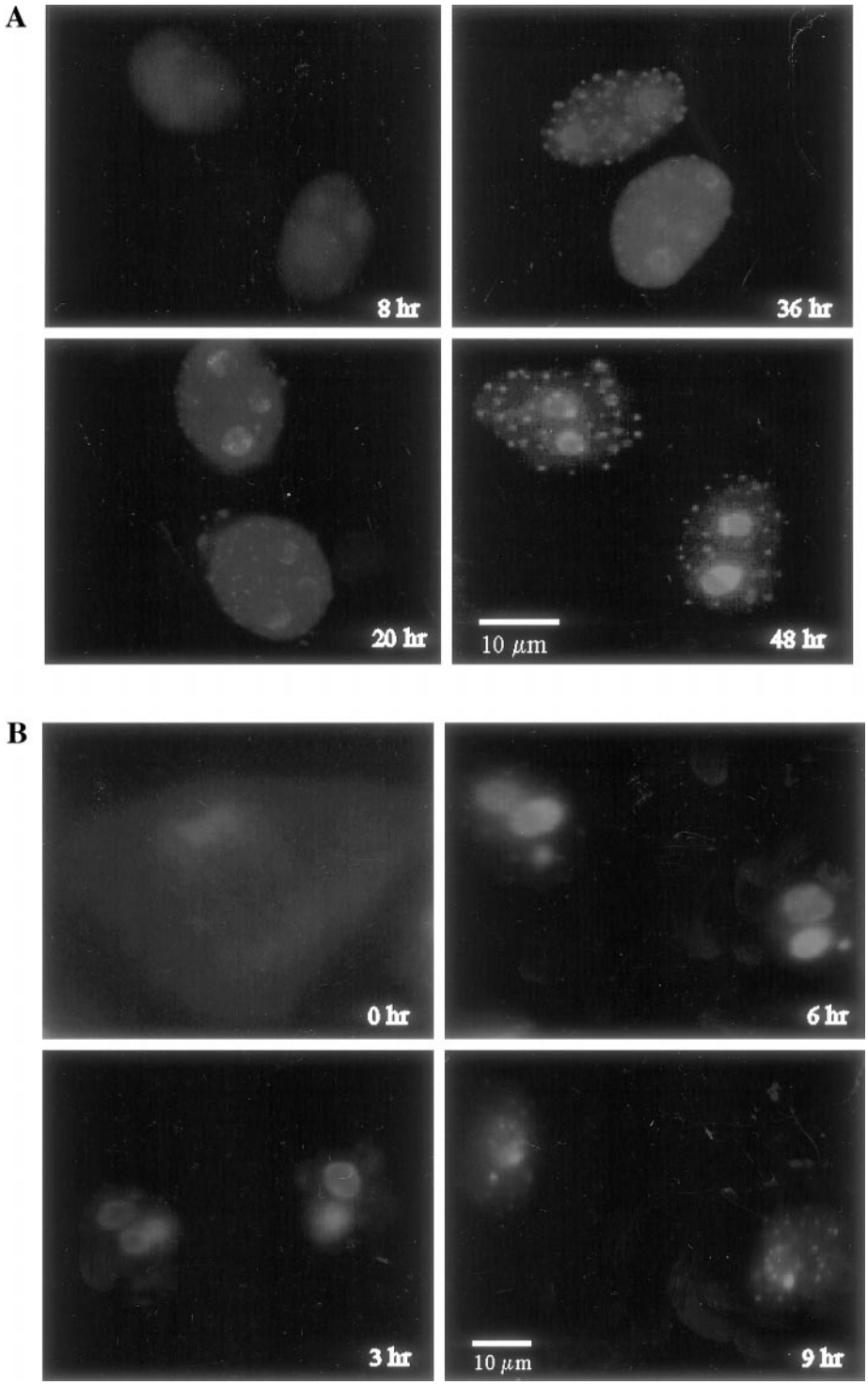


FIG. 7. Redistribution of GFP–LD. (A) Posttransfection fluorescence pattern of GFP–LD after transient transfection of pGFP–LD into HeLa cells. Times posttransfection are 8, 20, 36, and 48 h as indicated. (B) Postmitotic distribution of GFP–LD in permanently expressing HeLa cells. Times of postmitosis are 0, 3, 6, and 9 h as indicated. The scale bar represents 10 $\mu$m.

ability to inhibit HDV RNA replication (Fig. 5A), the nucleolus is thus suggested to be the site for HDV replication. This suggestion is supported by the finding that HDV anti-genome synthesis is insensitive to $\alpha$-amanitin (Modahl *et al.,* 2000) and that SDAg associates with nucleolin (Lee *et al.,* 1998). The current data also suggest that isoprenylation may not be required for *trans*-inhibitory activity (Fig. 5A, lane 6), which does not agree with previous observations (Hwang and Lai, 1994). Since different versions of non-prenylated LDAg could behave differently depending on their conformations (Hwang and Lai, 1994), the *trans*-inhibitory domain of GFP–LDM fu-

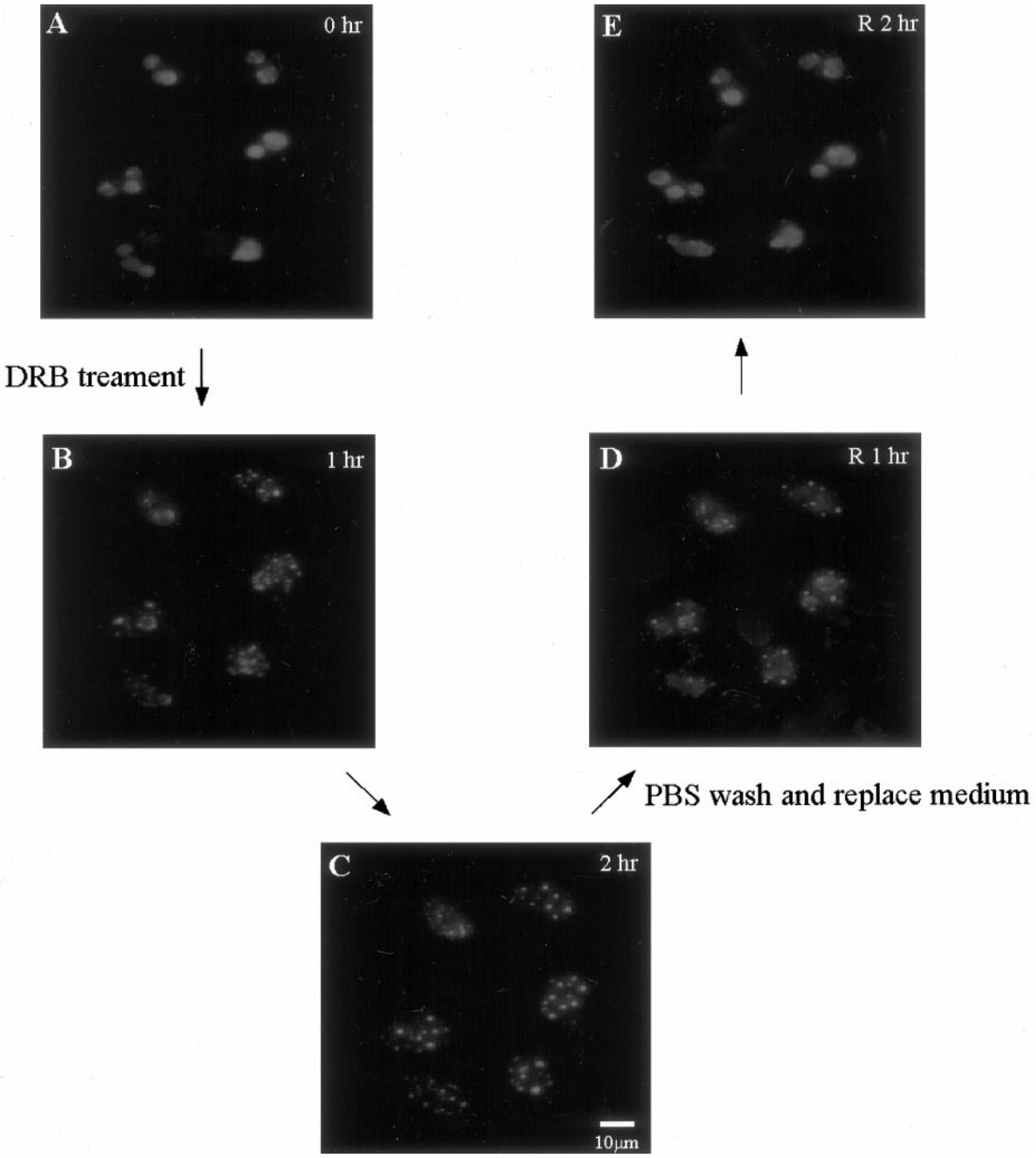


FIG. 8. Fluorescence pattern of GFP–LD after treatment with DRB and removal of the DRB. Before DRB treatment, the GFP–LD is located mainly in the nucleolus (0 h, A). After 1 or 2 h of DRB treatment, the GFP–LD appears in a speckled form (B and C). The nucleolus pattern resumes after DRB removal and its replacement with fresh medium (D and E are indicated with R 1 h and R 2 h). The scale bar represents 10 $\mu$m.

sion may remain as exposed as that of LDAg and GFP–LD, allowing interaction.

One great advantage that GFP offers is the study of the dynamic distribution of a fusion protein of interest in living cells under different physiological conditions. In this study, we treated GFP–LD cells with lovastatin and DRB, although both have a pleiotropic effect on cell metabolism, to demonstrate the dynamic distribution of GFP–LD (Figs. 6 and 8). One might argue that the dynamic distribution of GFP–LD was not directly due to GFP–LD modification. However, comparing the distribution pattern of lovastatin treatment of GFP–LD expressing cells with the GFP–LDM expressing cells, we suggest that isoprenylation is important for LDAg targeting to the NS with PML. Since the same concentration of DRB (100 $\mu$M) was used in this study as in the previous study (Yeh *et al.,* 1996), translocation of GFP–LD to the SC-35 containing NS (Fig. 9) is very likely due to the dephosphorylation of GFP–LD. The coexistence of HDAg with PML and SC-35 in NS has been previously reported and

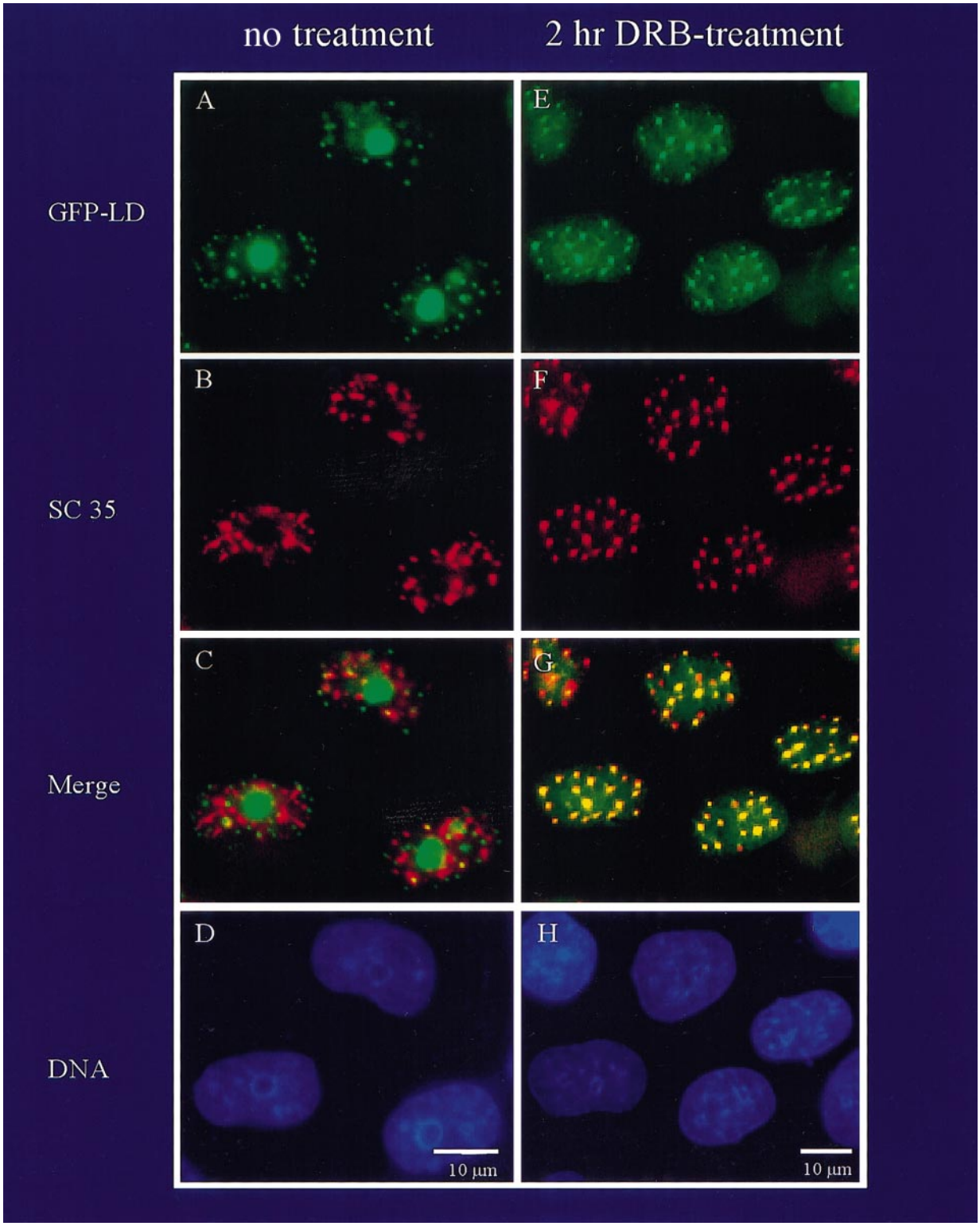


FIG. 9. Fluorescence pattern of GFP–LD and SC-35 in GFP–LD cells treated with (the right column) or without (the left column) DRB. (A and E) GFP pattern; (B and F) SC 35 pattern; (C and G) merged pictures of A + B and E + F; and (D and H) DNA staining. The merged pictures show that only a few speckled spots display GFP–LD coexisting with SC-35 in untreated cells while 90% of speckles show colocalization of GFP–LD with SC-35 (shown in yellow) in the DRB-treated cells. The scale bar represents 10 $\mu$m.

this was used to suggest that the SC-35 NS are the site for HDV replication (Bichko and Taylor, 1996). Although the mechanism and function of the shuttling between the two different types of NS and the nucleolus are not known, this study is the first to demonstrate that LDAg can be located in different compartments when it is

modified differently. However, the current observation is inconsistent with previous findings that the LDAg can be detected only in the nucleolus when anti-farnesyl antibody staining is used (Lin *et al.,* 1999). The discrepancy could be due to the insensitivity of the anti-farnesyl antibody stain as a method of detecting LDAg located in the speckle when the amount of LDAg is small. Alternatively, when the LDAg is transported to the speckle, the conformation of LDAg may be changed such that the isoprenylation site is hidden and can no longer be stained. These two hypotheses were based on the negative results of anti-farnesyl antibody staining on the GFP–LD expressing cells (data not shown). Nevertheless, both experiments demonstrate that prenylated LDAg can be present inside the nucleus.

In summary, by using GFP–fusion protein of HDV LDAg, in this study we have shown that the known biological functions of LDAg are not interfered with by fusion with GFP. This is also the first demonstration that the isoprenylation of LDAg can target it to the PML-containing NS and that dephosphorylation of LDAg is important for targeting to the SC-35 NS. Whether the sequential accumulation of GFP–LD is correlated with the modification and functions of LDAg needs further study. Nevertheless, different versions of GFP–fusion proteins can be used for dynamic studies in the future. It will be interesting to know whether or not coexpression of HBsAg and GFP–LD will change the general distribution pattern of GFP–LD.

## MATERIALS AND METHODS

### Plasmid construction

The eukaryotic expression vector pEGFP-C3, which contains the jellyfish gene of GFP, was obtained from Clontech Laboratories, Inc. (Palo Alto, CA). The coding region of full-length HDV LDAg was first generated by PCR using a primer containing a Kozak sequence and cloned into pGEMT to give pGEMT-L. The full-length HDV LDAg fragment was then excised from pGEMT-L and inserted into the *Bgl*II and *Eco*RI sites of pEGFP-C3, resulting in pGFP–LD. The pGFP–LDM plasmid containing a single mutation at the C-terminal cysteine of LDAg was generated in a similar manner except that a primer containing a mutation of Cys210 was used. Plasmids pGFP–LD(31-214) and pGFP–LD(31-214)M were constructed by inserting the HDV *Xho*I–*Eco*RI DNA fragments from the previously established pGEM3(−)-L and pGEMLm (Hu *et al.,* 1996) into pEGFP-C3. The plasmid of pCMVDag2 was derived from pSVL-d2g (Yeh *et al.,* 1996) in which a CMV promoter replaces the SV40 T antigen promoter to drive the dimer of 1.7-kb HDV cDNA and to produce an anti-genome of HDV RNA. Other non-GFP-containing plasmids, including pMTS, pMTLD, and pMTSD, were described previously (Sheu and Lo, 1992; Sheu *et al.,* 1996).

### Cell culture and transfection of HuH-7 and HeLa cells

Two human cell lines were used for plasmid transfection in this study. One is a well-differentiated human hepatoma cell line, HuH-7 (Nakabayashi *et al.,* 1982), and the other is epitheloid carcinoma cell line, HeLa (Eagle, 1955). Both cells were cultured in Dulbecco's modified Eagle's medium supplemented with 10% fetal bovine serum, penicillin (100 IU/ml), streptomycin (100 $\mu$g/ml), Fungizone (50 $\mu$g/ml), and 2 mM L-glutamine and grown at 37°C under 5% $CO_2$. Plasmids in a supercoiled form were obtained using the Qiagen Plasmid Maxi Kit (Hilden, Germany) and then used for transfection. For the packaging study, HuH-7 cells at 60% confluence in a 10-cm petri dish were cotransfected with 10 $\mu$g of plasmid pMTS, an HBsAg expression plasmid, and 10 $\mu$g of a plasmid encoding the wild-type LDAg, GFP–LD, GFP–LDM, GFP–LD(31-214), or GFP–LD(31-214)M by the calcium phosphate–DNA precipitation method (Graham and van der Eb, 1973). For generation of permanently expressing cell lines, the transfected HeLa cells were scraped off, reseeded to 10-cm plates, and selected with G418 (1 mg/ml) (Gibco BRL). Single colonies were then generated by limited dilution cloning.

### Fluorescence microscopy

Transiently or permanently transfected cells that express GFP–LD or other variants were cultured on 22 × 22 mm coverslips. Cells were fixed with 4% paraformaldehyde/PBS for 30 min at room temperature, stained first with anti-nucleolin antibody (Chen *et al.,* 1991), and then stained with the secondary goat-anti-mouse antibody conjugated with rhodamine. Thereafter cells were stained with Hoechst 33258, mounted on glass slides with mounting solution, and visualized with a fluorescence microscope (Olympus B-Max 60) or a confocal microscope (Leitz). For visualization of the dynamic distribution of the GFP–fusion proteins in transiently transfected cells or permanent cells treated with drugs (50 $\mu$M lovastain or 100 $\mu$M DRB), cells were examined using the Olympus B-Max 60 microscope and photographed.

### Nuclear extract and sucrose gradient

Permanently transfected cells were washed twice with PBS, scraped off from the culture dish, and collected by centrifugation. Cells were resuspended in 0.5 ml PBS and then lysed by the addition of 0.5 ml of 2% Triton X-100/PBS on ice. After 1 min, the cell lysates were centrifuged at 3000 rpm for 1 min to obtain the insoluble nuclear pellets, which were resuspended into 0.5 ml PBS and homogenized by sonication. The sonicated nuclear extracts (0.8 ml) were layered over a 10–50% (w/v) discontinuous sucrose gradient made up of sucrose in NET buffer [150 mM NaCl, 0.5 mM EDTA, 50 mM Tris–Cl (pH

7.5)] and then subjected to centrifugation at 38,000 rpm in an SW41 rotor (Beckman) for 16 h at 4°C. The gradients were fractionated into 18 0.6-ml samples and the density of each fraction was determined from the refractive index using a refractometer.

### Western blotting

Protein samples were separated by SDS–PAGE (Laemmli, 1970) and electrotransferred onto PVDF membranes (Immuobilon-P, Millipore) as described by Towbin *et al.* (1979). The membranes were first incubated with 5% nonfat milk and then with human anti-HDAg sera (Yeh *et al.,* 1996) or anti-nucleolin (Chen *et al.,* 1991) as alternative primary antibodies and then with horseradish peroxidase-conjugated anti-human antibody as the secondary antibody. The blot was detected by enhanced chemiluminescence (ECL Kit, Amersham Japan, Tokyo, Japan) or developed using 4-choloro-1-naphtol as the substrate.

### Northern blotting

Total RNA was extracted from transfected HeLa cells using the REnol C&T kit (PROtech Technologies, Inc.) following the protocol from the supplier. RNA samples (20 $\mu$g) were electrophoresed on a 1% RNA agarose gel and then transferred to nylon membrane by the capillary method (Sambrook *et al.,* 1989). The membrane was crosslinked using the UV Stratalinker 2400 (Stratagene), followed by prehybridization with Ultrasensitive Hybridization buffer (Ambion) and hybridization with $^{32}$P-labeled HDV-specific DNA probe. The filter was finally exposed to the Molecular Dynamic Storage Phosphor Screen.

## ACKNOWLEDGMENTS

We are indebted to Drs. M. M. C. Lai and Y.-H. W. Lee for providing us with the HDV cDNA containing plasmids, to Dr. M.-S. Shiao for the gift of lovastatin, to Dr. N.-S. Yeh for the monoclonal antibody against human nucleolin, and to Dr. W.-J. Syu for the anti-farnesyl antibody. Thanks are also due to Dr. Y.-H. W. Lee for her long-term discussions on the HDV work as well as for access to her unpublished data and to Dr. R. Kirby (a visiting professor of the Institute of Genetics) for editing the English in this article. This work was supported by grants from the National Science Council (NSC88-2314-B-010-059 and NSC89-2320-B-010-021-Y). S.J.L. was a research awardee from the National Science Council and the Medical Research and Advancement Foundation in Memory of Dr. Chi-Shuen Tsou.

## REFERENCES

Bell, P., Brazas, R., Ganem, D., and Maul, G. G. (2000). Hepatitis delta virus replication generates complexes of large hepatitis delta antigen and antigenomic RNA that affiliate with and alter nuclear domain 10. *J. Virol.* **74,** 5329–5336.

Bichko, V., and Taylor, J. M. (1996). Redistribution of the delta antigens in cells replicating the genome of hepatitis delta virus. *J. Virol.* **70,** 8064–8070.

Bichko, V., Barik, S., and Taylor, J. (1997). Phosphorylation of the hepatitis delta virus antigens. *J. Virol.* **71,** 512–518.

Bonino, F., Heermann, K. H., Rizzetto, M., and Gerlich, W. H. (1986). Hepatitis delta virus: Protein composition of delta antigen and its hepatitis B virus-derived envelope. *J. Virol.* **58,** 945–950.

Boundonck, K., Dolan, L., and Shaw, P. J. (1999). The movement of coiled bodies visualized in living plant cells by the green fluorescent protein. *Mol. Biol. Cell* **10,** 2297–2307.

Casey, J. L., Bergmann, K. F., Brown, T. L., and Gerin, J. L. (1992). Structural requirements for RNA editing in hepatitis delta virus: Evidence for a uridine-to-cytidine editing mechanism. *Proc. Natl. Acad. Sci. USA* **89,** 7149–7153.

Chang, F.-L., Chen, P.-J., Tu, S.-J., Wang, C.-J., and Chen, D.-S. (1991). The large form of hepatitis $\delta$ antigen is crucial for assembly of hepatitis $\delta$ virus. *Proc. Natl. Acad. Sci. USA* **88,** 8490–8494.

Chang, M.-F., Baker, S. C., Soe, L. H., Kamahora, T., Keck, J. G., Makino, S., Govindarajan, S., and Lai, M. M. C. (1988). Human hepatitis delta antigen is a nuclear phosphoprotein with RNA-binding activity. *J. Virol.* **62,** 2403–2410.

Chang, M.-F., Chang, S. C., Chang, C.-I., Wu, K., and Kang, H.-Y. (1992). Nuclear localization signals, but not putative leucine zipper motif, are essential for nuclear transport of hepatitis delta antigen. *J. Virol.* **66,** 6019–6027.

Chang, M.-F., Sun, C.-Y., Chen, C.-J., and Chang, S. C. (1993). Functional motifs of delta antigen essential for RNA binding and replication of hepatitis delta virus. *J. Virol.* **67,** 2529–2536.

Chang, M.-F., Chen, C.-H., Lin, S.-L., Chen, C.-J., and Chang, S. C. (1995). Functional domains of delta antigens and viral RNA required for RNA packaging of hepatitis delta virus. *J. Virol.* **69,** 2508–2514.

Chao, M., Hsieh, S.-Y., and Taylor, J. (1990). Role of two forms of hepatitis delta virus antigen: Evidence for a mechanism of self-limiting genome replication. *J. Virol.* **64,** 5066–5069.

Chen, C.-M., Chiang, S.-Y., and Yeh, N.-H. (1991). Increased stability of nucleolin in proliferating cells by inhibition of its self-cleaving activity. *J. Biol. Chem.* **266,** 7754–7758.

Chen, P.-J., Kalpana, G., Goldberg, J., Mason, W., Werner, B., Gerin, J., and Taylor, J. (1986). Structure and replication of the genome of the hepatitis delta virus. *Proc. Natl. Acad. Sci. USA* **83,** 8774–8778.

Chen, P.-J., Chang, F.-L., Wang, C.-J., Lin, C.-J., Sung, S.-Y., and Chen, D.-S. (1992). Functional study of hepatitis delta virus large antigen in packaging and replication inhibition: Role of the amino-terminal leucine zipper. *J. Virol.* **66,** 2853–2859.

Eagle, H. (1955). Nutrition needs of mammalian cells in tissue culture. *Science* **122,** 501–504.

Glenn, J. S., Watson, J. A., Havel, C. M., and White, J. M. (1992). Identification of a prenylation site in delta virus large antigen. *Science* **256,** 1331–1333.

Graham, E. L., and van der Eb, A. J. (1973). A new technique for the assay of infectivity of human adenovirus 5 DNA. *Virology* **52,** 456–467.

Grosset, C., Chen, C.-Y. A., Xu, N., Sonenberg, N., Jacquemin-Sablon, H., and Shyu, A.-B. (2000). A mechanism for translationally coupled mRNA turnover: Interaction between the poly(A) tail and a *c-fos* RNA coding determinant via a protein complex. *Cell* **103,** 29–40.

Hu, H.-M., Shih, K.-N., and Lo, S. J. (1996). Disulfide bond formation of the *in vitro*-translated large antigen of hepatitis D virus. *J. Virol. Methods* **60,** 39–46.

Huang, W.-H., Yung, B. Y. M., Syu, W. J., and Lee, Y.-H. W. (2001). The nucleolar phosphoprotein B23 interacts with hepatitis delta antigens and modulates the hepatitis delta virus RNA replication. *J. Biol. Chem.,* in press.

Hwang, S. B., Lee, C.-Z., and Lai, M. M. C. (1992). Hepatitis delta antigen expressed by recombinant baculoviruses: Comparison of biochemical properties and post-translational modifications between the large and small forms. *Virology* **190,** 413–422.

Hwang, S. B., and Lai, M. M. C. (1994). Isoprenylation masks a conformational epitope and enhances *trans*-dominant inhibitory function of the large hepatitis delta antigen. *J. Virol.* **68,** 2958–2964.

Ivessa, N. E., Gravotta, D., De Lemos-Chiarandini, C., and Kreibich, G. (1997). Functional protein prenylation is required for the brefeldin

A-dependent retrograde transport from the Golgi apparatus to the endoplasmic reticulum. *J. Biol. Chem.* **272,** 20828–20834.

Kos, A., Dijkema, R., Arnberg, A. C., van der Meide, P. H., and Schelekens, H. (1986). The hepatitis delta (δ) virus possesses a circular RNA. *Nature* **323,** 558–560.

Kuo, M. Y.-P., Chao, M., and Taylor, J. (1989). Initiation of replication of the human hepatitis delta virus genome from cloned DNA: Role of delta antigen. *J. Virol.* **63,** 1945–1950.

Laemmli, U. K. (1970). Cleavage of structural proteins during the assembly of the head of bacteriophage T4. *Nature* **227,** 680–685.

Lai, M. M. C. (1995). The molecular biology of hepatitis delta virus. *Annu. Rev. Biochem.* **64,** 259–286.

Lazinski, D. W., and Taylor, J. (1993). Relating structure to function in the hepatitis delta virus antigen. *J. Virol.* **67,** 2672–2680.

Lee, C.-H., Chang, S. C., Chen, C.-I., and Chang, M.-F. (1998). The nucleolin binding activity of hepatitis delta antigen is associated with nucleolus targeting. *J. Biol. Chem.* **273,** 7650–7656.

Lee, C.-Z., Chen, P.-J., Lai, M. M. C., and Chen, D.-S. (1994). Isoprenylation of large delta antigen is necessary but not sufficient for hepatitis delta assembly. *Virology* **199,** 169–175.

Lee, C.-Z., Chen, P.-J., and Chen, D.-S. (1995). Large hepatitis delta antigen in packaging and replication inhibition: Role of the carboxy-terminal 19 amino acids and amino-terminal sequences. *J. Virol.* **69,** 5332–5336.

Lin, H.-P., Hsu, S.-C., Wu, J.-C., Sheen, I.-J., Yan, B.-S., and Syu, W.-J. (1999). Localization of isoprenylated antigen of hepatitis delta virus by anti-farnesyl antibodies. *J. Gen. Virol.* **80,** 91–96.

Luo, G. X., Chao, M., Hsieh, S.-Y., Sureau, C., Nishikura, K., and Taylor, J. (1990). A specific base transition occurs on replicating hepatitis delta virus RNA. *J. Virol.* **64,** 1021–1027.

Makino, S., Chang, M.-F., Shieh, C.-K., Kamahora, T., Vannier, D. M., Govindarajan, S., and Lai, M. M. C. (1987). Molecular cloning and sequencing of a human hepatitis delta (δ) virus RNA. *Nature* **329,** 343–346.

Misteli, T., and Spector, D. L. (1997). Applications of the green fluorescent protein in cell biology and biotechnology. *Nat. Biotechnol.* **15,** 961–964.

Modahl, L. E., MacNaughton, T. B., Zhu, N., Johnson, D. L., and Lai, M. M. (2000). RNA-dependent replication and transcription of hepatitis delta virus RNA involve distinct cellular RNA polymerase. *Mol. Cell. Biol.* **20,** 6030–6039.

Moraleda, G., Seeholzer, S., Bichko, V., Dunbrack, R., Otto, J., and Taylor, J. (1999). Unique properties of the large antigen of hepatitis delta virus. *J. Virol.* **73,** 7147–7152.

Mu, J.-J., Wu, H.-L., Chiang, B.-L., Chang, R.-P., Chen, D.-S., and Chen, P.-J. (1999). Characterization of the phosphorylated forms and the phosphrylated residues of hepatitis delta virus delta antigens. *J. Virol.* **73,** 10540–10545.

Nakabayashi, H., Taketa, K., Miyano, K., Yamane, T., and Sato, J. (1982). Growth of human hepatoma cell lines with differentiated functions in chemically defined medium. *Cancer Res.* **42,** 3858–3863.

Ponzetto, A., Cote, P. J., Popper, H., Hoyer, B. H., London, W. T., Ford, E. C., Bonino, F., Purcell, R. H., and Gerin, J. L. (1984). Transmission of the hepatitis B virus-associated delta agent to the eastern woodchuck. *Proc. Natl. Acad. Sci. USA* **81,** 2208–2212.

Rizzetto, M. (1983). The delta agent. *Hepatology* **3,** 729–737.

Ryu, W.-S., Bayer, M., and Taylor, J. (1992). Assembly of hepatitis delta virus particles. *J. Virol.* **66,** 2310–2315.

Sakai, N., Sasaki, K., Ikegaki, N., Shirai, Y., Ono, Y., and Satio, N. (1997). Direct visualization of the translocation of the gamma-subspecies of protein kinase C in living cells using fusion proteins with green fluorescent protein. *J. Cell Biol.* **139,** 1465–1476.

Sambrook, J., Fritsch, E. F., and Maniatis, T. (1989). "Molecular Cloning: A Laboratory Manual," 2nd ed. Cold Spring Harbor Laboratory Press, Cold Spring Harbor, NY.

Sheu, S. Y., and Lo, S. J. (1992). Preferential ribosomal scanning is involved in the differential synthesis of the hepatitis B viral surface antigens from subgenomic transcripts. *Virology* **188,** 353–357.

Sheu, S. Y., Chen, K.-L., Lee, Y.-H. W., and Lo, S. J. (1996). No intermolecular interaction between the large hepatitis delta antigens is required for the secretion with hepatitis B surface antigen: A model of empty HDV particles. *Virology* **218,** 275–278.

Sinensky, M., Beck, L. A., Leonard, S., and Evans, R. (1990). Differential inhibitory effects of lovastatin on protein isoprenylation and sterol synthesis. *J. Biol. Chem.* **265,** 19937–19941.

Towbin, H., Staehelin, T., and Gordon, J. (1979). Electrophoretic transfer of proteins from polyacrylamide gels to nitrocellulose sheets: Procedure and some applications. *Proc. Natl. Acad. Sci. USA* **76,** 4530–4534.

Wang, C.-J., Chen, P.-J., Wu, J.-C., Patel, D., and Chen, D.-S. (1991). Small-form hepatitis B surface antigen is sufficient to help in the assembly of hepatitis delta virus-like particles. *J. Virol.* **65,** 6630–6636.

Wang, H.-W., Chen, P.-J., Lee, C.-Z., Wu, H.-L., and Chen, D.-S. (1994). Packaging of hepatitis delta virus RNA via the RNA-binding domain of hepatitis delta antigens: Different roles for the small and large delta antigens. *J. Virol.* **68,** 6363–6371.

Wang, J.-G., and Lemon, S. M. (1993). Hepatitis delta virus antigen forms dimers and multeric complexes *in vivo*. *J. Virol.* **67,** 446–454.

Wang, K.-S., Choo, Q.-L., Weiner, A. J., Ou, J.-H., Najarian, R. C., Thayer, R. M., Mullenbach, G. T., Denniston, K. J., Gerin, J. L., and Houghton, M. (1986). Structure, sequence and expression of the hepatitis delta (δ) viral genome. *Nature* **323,** 508–514.

Weiner, A. J., Choo, Q.-L., Wang, K.-S., Govindarajan, S., Redeker, A. G., Gerin, J. L., and Houghton, M. (1988). A single antigenomic open reading frame of the hepatitis delta virus encodes the epitope(s) of both hepatitis delta antigen polypeptides $p24^{\delta}$ and $p27^{\delta}$. *J. Virol.* **62,** 594–599.

White, J., and Stelzer, E. (1999). Photobleaching GFP reveals protein dynamics inside live cells. *Trends Cell Biol.* **9,** 61–65.

Wu, J.-C., Chen, C.-L., Lee, S.-D., Sheen, I.-J., and Ting, L.-P. (1992). Expression and localization of the small and large delta antigens during the replication cycle of hepatitis D virus. *Hepatology* **16,** 1120–1127.

Xia, Y.-P., Yeh, C.-T., Ou, J.-H., and Lai, M. M. C. (1992). Characterization of nuclear targeting signal of hepatitis delta antigen: Nuclear transport as a protein complex. *J. Virol.* **66,** 914–921.

Xia, Y.-P., and Lai, M. M. C. (1992). Oligomerization of hepatitis delta antigen is required for both the *trans*-activating and *trans*-dominant inhibitory activities of the delta antigen. *J. Virol.* **66,** 6641–6648.

Yeh, T.-S., Lo, S. J., Chen, P.-J., and Lee, Y.-H. W. (1996). Casein kinase II and protein kinase C modulate hepatitis delta virus RNA replication but not empty viral particle assembly. *J. Virol.* **70,** 6190–6198.

Zheng, E., Fu, T.-B., Lanzinski, D., and Taylor, J. (1992). Editing on the genomic RNA of human hepatitis delta virus. *J. Virol.* **66,** 4693–4697.

Zuccola, H. J., Rozzelle, J. E., Lemon, S. M., Erickson, B. W., and Hogle, J. M. (1998). Structural basis of the oligomerization of hepatitis delta antigen. *Structure* **15,** 821–830.